Supporting Information

Inhomogeneous Strain Release during Bending of WS_2 on Flexible Substrates

Martin E. P. Tweedie[†], Yuewen Sheng[†], Syed Ghazi Sarwat[‡], Wenshuo Xu[†], Harish Bhaskaran[‡], Jamie H. Warner[†]*

[†]Nanostructured Materials Group, Department of Materials, University of Oxford, Parks Road, Oxford, OX1 3PH, United Kingdom

[‡] Advanced Nanoscale Engineering Group, Department of Materials, University of Oxford, Parks Road, Oxford, OX1 3PH, United Kingdom

*jamie.warner@materials.ox.ac.uk;

Before Gaussian decomposition can be performed, spectra must be converted from wavelength to eV, using the equation [1]:

$$E = \frac{hc}{\lambda} \qquad [1]$$

Where E is energy, h is the Planck constant, c is the speed of light, and λ is wavelength. In addition, the intensity (I) must be rescaled by the Jacobian transformation [2]:[1]

$$I_E = \frac{I_\lambda hc}{E^2} \qquad [2]$$

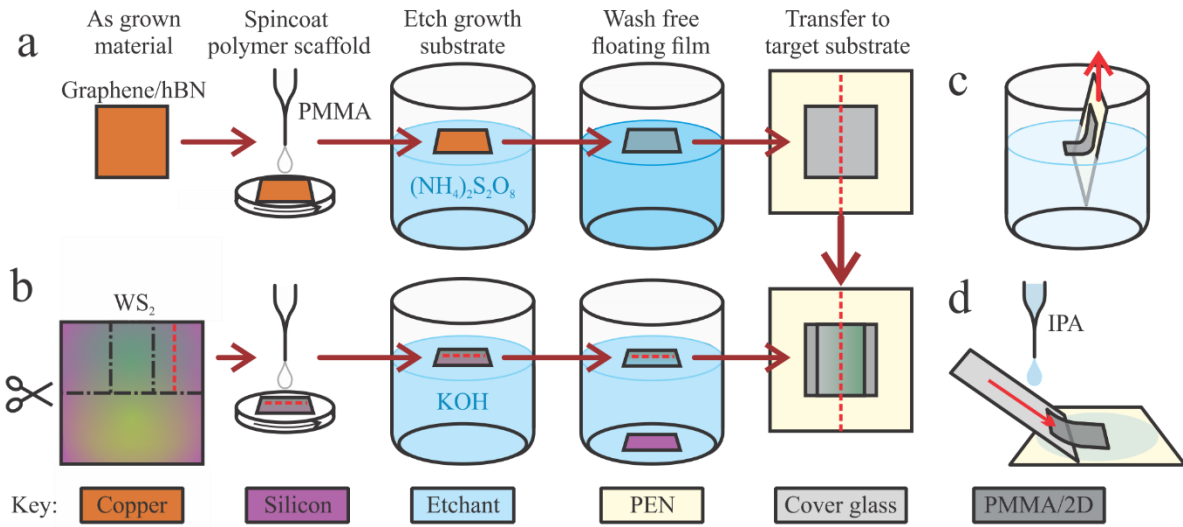Once this has been performed, the spectra can be decomposed into their various contributions.

Figure S1: Details of the transfer process for (a) graphene and hBN and (b) WS$_2$, showing how the heterostructure is built up on the substrate. As grown materials were spincoated with a 500 nm PMMA scaffold prior to etching, washed in DI water, and transferred sequentially to the substrate. The chain lines in (b) show how the wafer is diced to select the area of highest quality WS$_2$, and the red dashed line indicates the alignment of the best domains with the centre line of the substrate. Transfer by the (c) wet/aqueous process, in which the floating film is picked up directly onto the substrate; and (d) non-

aqueous process, where the film is first picked up on an intermediate support before being moved to the target substrate using isopropyl alcohol (IPA).
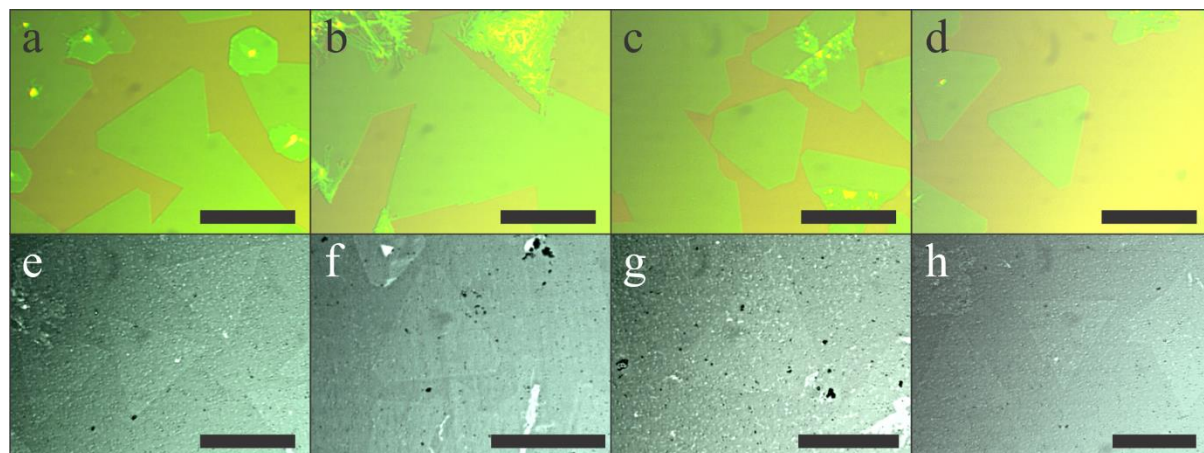

Figure S2: False colour optical images of WS$_2$ domains (a-d) before and (e-h) after transfer to PEN substrate, showing some of the shapes possible and the retained sharp edges of the domains after transfer. Scale bar is 100 μm.
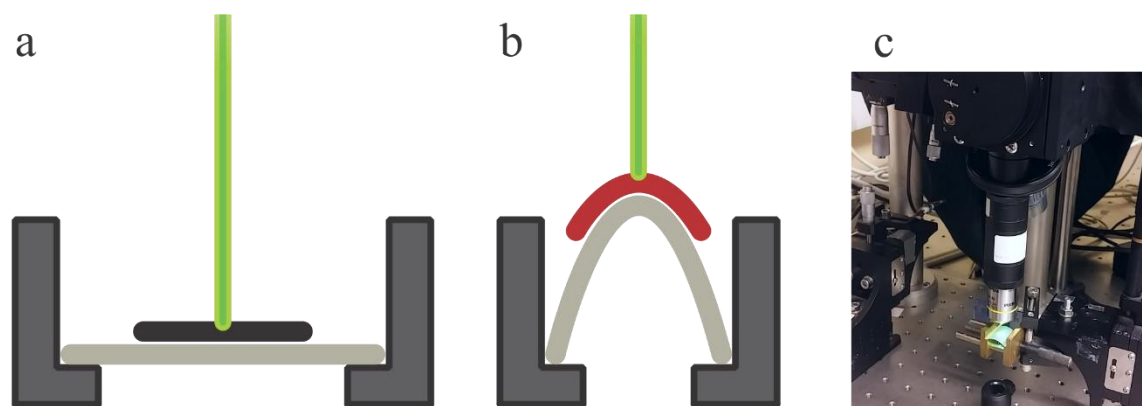

Figure S3: Schematics of the strain holder in (a) relaxed and (b) strained positions, and (c) picture of holder in place in spectrometer.
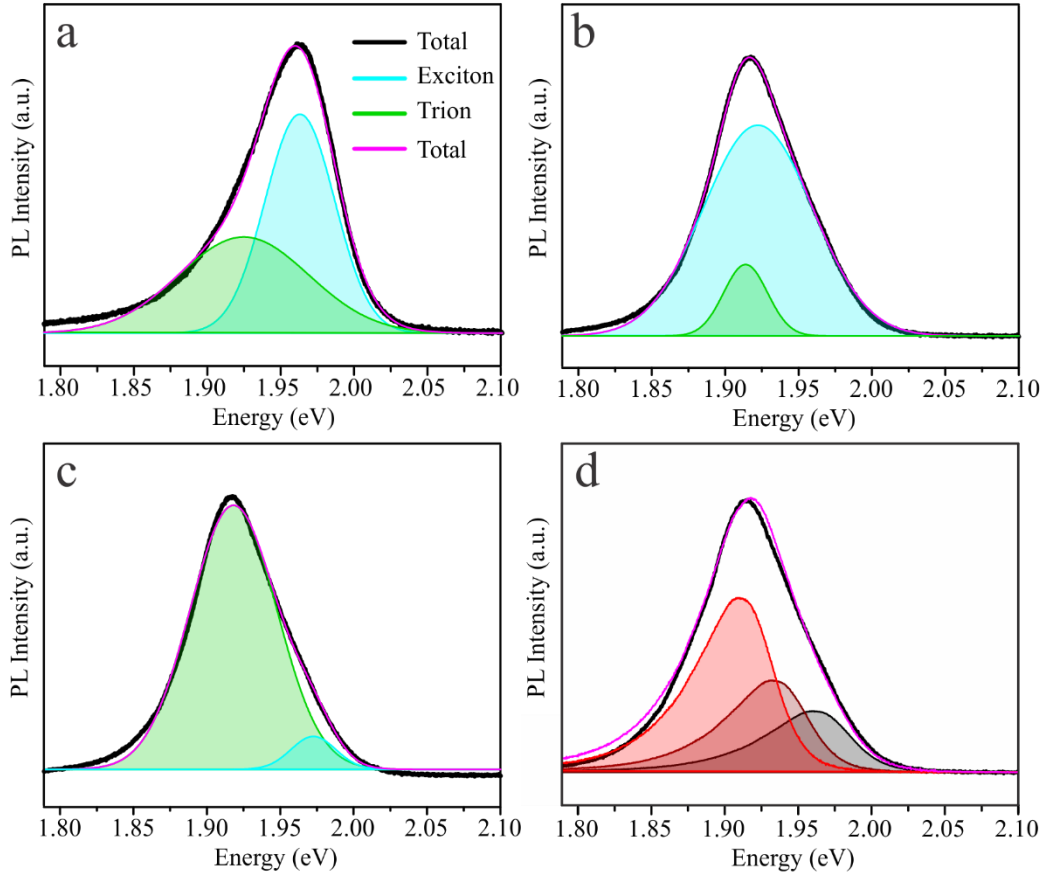
Figure S4: Typical PL spectra taken during the 1st strain cycle. At 0 % strain (a), the peak shape is as expected for WS_2 and the Gaussian decomposition is valid. At higher strains the peak shape becomes distorted and the fitting was judged to have failed due to discontinuities compared to the fitting of prior and successive spectra, typically as shown in (b) but also as shown in (c). (d) Artificially stacking the spectrum from (a) shifted across several different energies produces a good approximation of the peak shape in (b). This provides evidence for the hypothesis of inhomogeneous strain in the WS_2 leading to emission from a distribution of bandgaps.
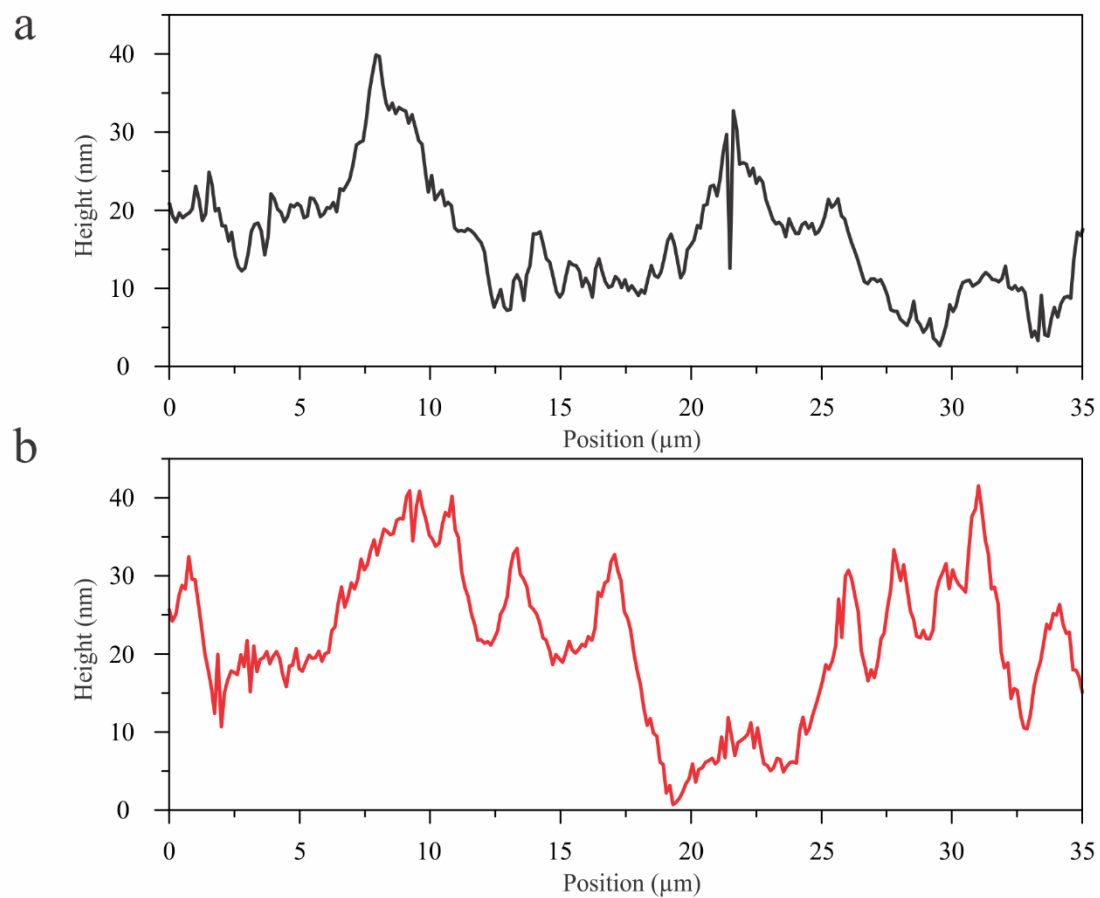
Figure S5: Typical line profiles from the WS$_2$/graphene/PEN aq surface, taken by atomic force microscopy (a) before and (b) after the application of strain, from different but comparable areas.
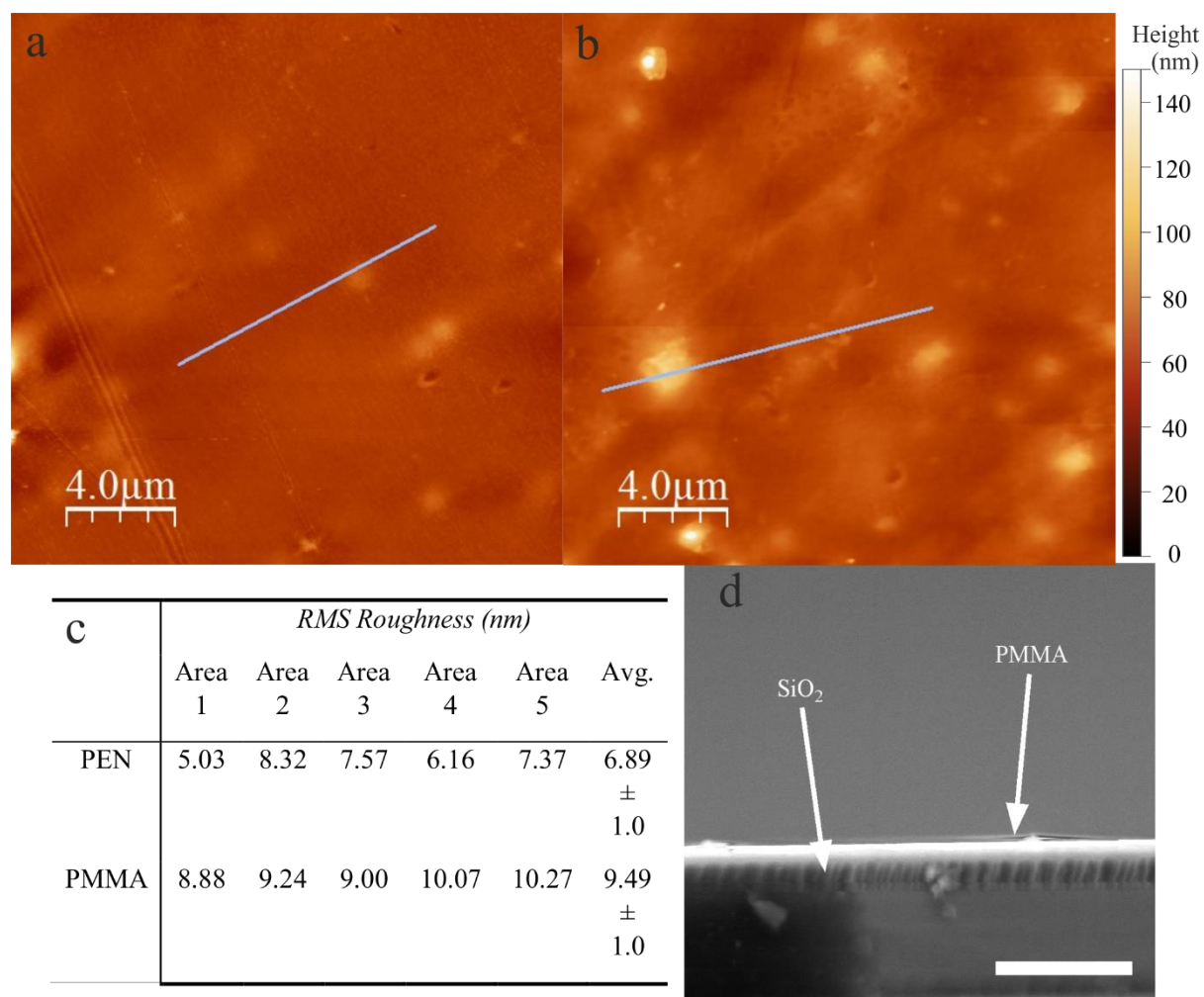
Figure S6: Characterisation of the surface topography and roughness for the PEN substrate with and without PMMA coating. Example AFM images taken on PEN (a) without and (b) with a layer of A1 495K PMMA spin coated onto the surface, and (c) a chart summarising the RMS roughness values of multiple line profiles take from both. (d) Example of cross sectional SEM image of the 50 ± 5 nm PMMA layer deposited by the same parameters onto a silicon wafer with 300 nm oxide layer, used in determining the film thickness. Scale bar is 1 μm.
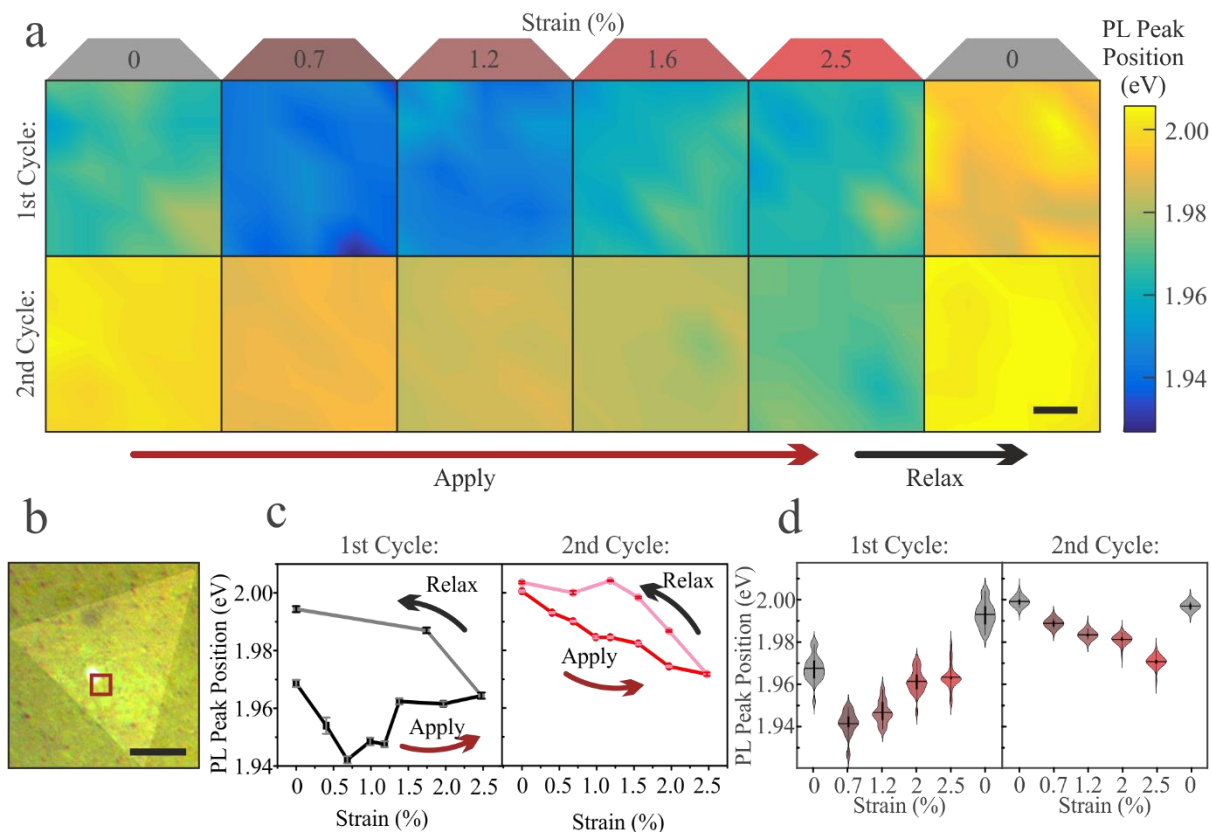
c

	RMS Roughness (nm)					
	Area 1	Area 2	Area 3	Area 4	Area 5	Avg.
PEN	5.03	8.32	7.57	6.16	7.37	6.89 ± 1.0
PMMA	8.88	9.24	9.00	10.07	10.27	9.49 ± 1.0

Figure S7: Local mapping of the peak shifts during the first strain cycle on the WS_2/graphene/PMMA/PEN aq heterostructure, as demonstrated for WS_2/graphene/PEN non-aq in Figure 5. (a) Maps of PL peak positions during the first and second cycle, as strain is applied and relaxed. Scale indicated in the last frame is 2 μm. (b) False colour micrograph with mapping area indicated. Scale bar is 20 μm. (c) Average peak positions at each strain position for the first and second cycle, and (d) violin plots showing the distribution of peak positions within the mapped area. Note similar large-scale shift and release during first strain cycle and comparatively small shifts during second cycle, accompanied by a reduction in the spread of the data in the second cycle, with a later and broader onset of debonding and greater distribution of peak positions in the 1st cycle than the WS_2/graphene/PEN non-aq heterostructure.

References

(1) Kambhamptai, P. Get the Basics Right: Jacobian Conversion of Wavelength and Energy Scales for Quantitative Analysis of Emission Spectra. *Journal of Physical Chemistry Letters* **2013**, *4*, 3316–3318.